# Optimal Feedback Guidance of a Small Aerial Vehicle in the Presence of Stochastic Wind

Ross P. Anderson[1]
*University of California, Santa Cruz, CA*

Efstathios Bakolas[2]
*University of Texas at Austin, Austin, TX*

Dejan Milutinović[3]
*University of California, Santa Cruz, CA*

Panagiotis Tsiotras[4]
*Georgia Institute of Technology, Atlanta, GA*

**The navigation of a small unmanned aerial vehicle is challenging due to a large influence of wind to its kinematics. When the kinematic model is reduced to two dimensions, it has the form of the Dubins kinematic vehicle model. Consequently, this paper addresses the problem of minimizing the expected time required to drive a Dubins vehicle to a prescribed target set in the presence of a stochastically varying wind. First, two analytically-derived control laws are presented. One control law does not consider the presence of the wind, whereas the other assumes that the wind is constant and known a priori. In the latter case it is assumed that the prevailing wind is equal to its mean value; no information about the variations of the wind speed and direction is available. Next, by employing numerical techniques from stochastic optimal control, feedback control strategies are computed. These anticipate the stochastic variation of the wind and drive the vehicle to its target set while minimizing the expected time of arrival. The analysis and numerical simulations show that the analytically-derived de-**

[1] Graduate Student, Department of Applied Mathematics and Statistics, Email: anderson@soe.ucsc.edu
[2] Assistant Professor, Department of Aerospace Engineering, Email: bakolas@austin.utexas.edu. Member AIAA
[3] Assistant Professor, Department of Applied Mathematics and Statistics, Email: dejan@soe.ucsc.edu
[4] Professor, School of Aerospace Engineering, Email: tsiotras@gatech.edu. Fellow AIAA

**terministic optimal control for this problem captures, in many cases, the salient features of the optimal feedback control for the stochastic wind model, providing support for the use of the former in the presence of light winds. On the other hand, the controllers anticipating the stochastic wind variation lead to more robust and more predictable trajectories than the ones obtained using feedback controllers for deterministic wind models.**

### Nomenclature

$(x, y)$ = Cartesian coordinates of the position vector of the Dubins vehicle, m

$\theta$ = heading angle of the Dubins vehicle, rad

$r$ = distance to target, m

$\delta$ = target set radius, m

$\varphi$ = viewing angle to target, rad

$\gamma$ = difference in Dubins vehicle heading angle and wind direction, rad

$u$ = control input, rad m/s

$v$ = Dubins vehicle speed, m/s

$\rho_{\min}$ = Dubins vehicle minimum turning radius, m

$\mathrm{d}W_{x,y}$ = increments of Wiener process in, respectively, the $x$ and $y$ direction

$\mathrm{d}W_{\theta}$ = increments of Wiener process in the $\theta$ direction

$\sigma_W$ = noise intensity for first wind model, m

$v_w$ = speed of wind in second wind model, m/s

$\sigma_\theta$ = noise intensity for second wind model, rad

$T$ = time-to-go until the target set is reached, s

## I. Introduction

This paper deals with the problem of guiding an aerial vehicle with a turning rate constraint to a prescribed terminal position in the presence of a stochastic wind in minimum expected time.

It is assumed that the motion of the vehicle is described by a Dubins-like kinematic model [1–3], that is, it travels only forward with constant speed, and such that the rate of change of its forward velocity vector direction is bounded by a prescribed upper bound. This kinematic model is referred to as the Dubins Vehicle (DV for short). In the absence of the wind, the vehicle traverses paths of minimal length and bounded curvature, known in the literature as Dubins paths or optimal paths of the Markov-Dubins (MD for short) problem [1, 4].

The importance of designing trajectory tracking control schemes and path planning algorithms that account for the effects of the local wind in UAVs/MAVs applications has been recognized by many researchers. In particular, Refs. [5–8] present path tracking/following controllers for UAVs/MAVs in the presence of disturbances induced by the wind based on nonlinear control tools. The problem of characterizing minimum-time paths of a DV in the presence of a constant wind was first posed by McGee and Hedrick in [9]. Numerical schemes for the computation of the Dubins-like paths proposed in [9] have been presented in [10, 11]. The complete characterization of the optimal solution of the same problem, that is, a mapping that returns the minimum-time control input given the state vector of the DV, is given in [11, 12]. A numerical algorithm that computes the minimum-time paths of the DV in the presence of a deterministic time-varying, yet spatially invariant, wind is presented in [13].

The analysis presented in the majority of the variations and extensions of the MD problem in the literature is based on a deterministic optimal control framework (the reader interested in a thorough literature review on variations/extensions of the MD problem may refer to [14] and references therein). The effect of the wind, however, is intrinsically stochastic, and approaching this problem from a stochastic point of view is more appropriate. Some recent attempts to address optimal control problems related to the MD problem within a stochastic optimal control framework can be found in [15, 16]. In particular, Refs. [15, 16] deal with the problem of a DV tracking a target with an uncertain future trajectory using numerical techniques from stochastic optimal control of continuous-time processes [17].

In this work, an optimal *feedback* control that minimizes the expected time required to navigate the DV to its prescribed target set in the presence of a stochastic wind is developed. Two stochastic

wind models are investigated. In the first model the $x$ and $y$ components of the wind are modeled as independent zero-mean Wiener processes with a given intensity level. In the second model, the wind is modeled as having a constant magnitude, but its direction is unknown and is allowed to vary stochastically according to a zero-mean Wiener process. For both wind models, optimal feedback control laws are computed numerically using a Markov chain approximation scheme. In addition, for each control based on the stochastic wind models, feedback control laws based on deterministic wind models are developed and compared against their stochastic model-based counterparts in the presence of stochasticity to determine the regions of validity of the former. The analysis and numerical simulations demonstrate, not surprisingly perhaps, that control laws based on stochastic wind models outperform – on the average – control laws for the deterministic wind models implemented in a stochastic wind. On the other hand, the control laws for the deterministic wind model can successfully capture the salient features of the structure of the corresponding stochastic optimal control solution.

The contributions of the paper can be summarized as follows: First, this paper offers, up to the authors' best knowledge, for the first time, the solution of the optimal path generation of an aerial vehicle with Dubins-like kinematics in the presence of stochastic wind. This is important for small UAV path-planning and coordination applications. Second, it shows the relationship of the optimal control solution, which anticipates the stochastic wind, with its deterministic counterpart, and it compares the two. This allows one to draw insights as to what level a stochastic wind-based solution is beneficial compared to its less informed deterministic counterpart, and when it makes sense (from a practical point of view) to use the former over the latter. The question of the use of a feedback control law anticipating stochastic processes versus a control law based on deterministic model assumptions is a question of a more general interest and one that is a recurrent theme in the community, especially in terms of applications. This paper offers a rare example where a head-to-head comparison is possible. In general, the computation of a deterministic optimal feedback control is not an easy task, as it requires the solution of a Hamilton-Jacobi-Bellman (HJB) partial differential equation. However, the Dubins vehicle problem in this paper serendipitously allows for a complete solution, via a synthesis of open-loop strategies, without resorting to the HJB equation.

The rest of the paper is organized as follows. Section II formulates the optimal control problem. Section III presents feedback control laws based on minimal deterministic and stochastic wind model assumptions. These control laws are extended in Section IV for the case when the wind has a known speed but stochastically-varying direction. Simulation results for the controllers based on the two types of deterministic and stochastic wind models are presented in Section V. Finally, Section VI concludes the paper with a summary of remarks.

## II. Problem Formulation

Here the problem of controlling the turning rate of a fixed-speed Dubins vehicle (DV) in order to reach a stationary target in the presence of wind is formulated. The target is fixed at the origin, while the Cartesian components of DV position are $x(t)$ and $y(t)$ (see Fig. 1).

[Fig. 1 about here.]

The DV moves in the direction of its heading angle $\theta$ at fixed speed $v$ relative to the wind and obeys the equations:

$$\mathrm{d}x(t) = v\cos(\theta)\,\mathrm{d}t + \mathrm{d}w_x(t,x,y), \tag{1}$$

$$\mathrm{d}y(t) = v\sin(\theta)\,\mathrm{d}t + \mathrm{d}w_y(t,x,y), \tag{2}$$

$$\mathrm{d}\theta(t) = \frac{u}{\rho_{\min}}\mathrm{d}t, \qquad |u| \le 1, \tag{3}$$

where $\rho_{\min} > 0$ is the minimum turning radius constraint (in the absence of wind) and $u$ is the control variable, $u \in [-1,1]$. The motion of the DV is affected by the spatially and/or temporally varying wind $w(t,x,y) = [w_x(t,x,y), w_y(t,x,y)]^\intercal$, whose increments have been incorporated into the model (1)-(2). In this problem formulation, the model for the wind is unknown. Therefore, it is assumed that the wind is described by a stochastic process. Subsequently, a stochastic control problem for reaching a target set $\mathcal{T} = \left\{(x,y) \,:\, x^2+y^2 \le \delta^2\right\}$, which is a ball of radius $\delta > 0$ around the target, is formulated.

In order to minimize the time required to reach the target set, one defines a cost-to-go function

$$J(\mathbf{x}) = \min_{|u|\le 1} \mathbf{E}\left[\int_0^T \mathrm{d}t\right], \qquad \mathbf{x} := [x(0), y(0), \theta(0)]^\intercal, \tag{4}$$

and assumes that upon reaching the target set $\mathcal{T}$ at time $T$, all motion ceases. In (4) the expected time to reach the target set is minimized over the turning rate $u$, $|u| \leq 1$, which is the control variable. Control problems with a cost-to-go function of the form (4) are sometimes referred to as "control until a target set is reached" [17] or stochastic shortest-path problems [18].

Two stochastic process wind models that are characterized by the amount of information known about the wind are considered. In each case, it is assumed that the wind is a continuous-time stochastic process with respect to the DV position. In other words, there is no explicit relation between a realization of the wind and the DV position, i.e., $w_x(t,x,y) = w_x(t)$, and $w_y(t,x,y) = w_y(t)$, although implicitly this relation may exist.

First, a feedback control when a model describing the wind is not given is developed. Drawing from the field of estimation, the simplest model to describe an unknown 2D signal suggests that the wind should be modeled as Brownian motion [19]. It is further assumed that the Cartesian components of the wind evolve independently. Then from (1)-(3), the kinematics of the DV in the presence of this wind, denoted model (W1), is

$$\begin{aligned} \mathrm{d}x(t) &= v\cos(\theta)\mathrm{d}t + \sigma_W \mathrm{d}W_x, \\ \mathrm{d}y(t) &= v\sin(\theta)\mathrm{d}t + \sigma_W \mathrm{d}W_y, \\ \mathrm{d}\theta(t) &= \frac{u}{\rho_{\min}}\mathrm{d}t, \qquad |u| \leq 1, \end{aligned} \tag{W1}$$

where $\mathrm{d}W_x$ and $\mathrm{d}W_y$ are mutually independent increments of a zero mean Wiener process, and where the level of noise intensity $\sigma_W$ quantifies the uncertainty in the evolution of the wind. Note that this kinematic model also arises when examining the problem of tracking a target with unknown future trajectory [15, 16]. In the limiting case where $\sigma_W = 0$, the problem is reduced to the case without the wind. A feedback control that assumes $\sigma_W = 0$, therefore, would ignore the presence of the wind, while a feedback control that assumes $\sigma_W > 0$ will account for the stochastic wind variation. Along these lines, Section III develops feedback control laws that drive the DV to the target in minimum time in both the deterministic case ($\sigma_W = 0$) and the stochastic case ($\sigma_W > 0$). Note that in the deterministic case, the cost-to-go function is the same as (4), but without the expectation operator.

Next, motivated by problems involving a wind that varies slowly in time and/or space, a second wind model (W2) is considered. The second wind model considers a wind that flows in the direction $\theta_w$ at constant speed $v_w < v$, but where the evolution of the direction of this wind is unknown. Then from (1)-(3), the model of the relative motion of the DV and the target in the wind (W2) is

$$\begin{aligned} \mathrm{d}x(t) &= v\cos(\theta)\,\mathrm{d}t + v_w\cos(\theta_w)\,\mathrm{d}t \\ \mathrm{d}y(t) &= v\sin(\theta)\,\mathrm{d}t + v_w\sin(\theta_w)\,\mathrm{d}t \\ \mathrm{d}\theta(t) &= \frac{u}{\rho_{\min}}\,\mathrm{d}t, \qquad |u| \le 1 \\ \mathrm{d}\theta_w(t) &= \sigma_\theta\,\mathrm{d}W_\theta, \end{aligned} \tag{W2}$$

where $\mathrm{d}W_\theta$ is an increment of a Wiener process, and where $\sigma_\theta$ is its corresponding intensity. When $\sigma_\theta = 0$, one obtains a model of constant wind in the direction $\theta_w$. Section IV describes optimal feedback controls for the deterministic case ($\sigma_\theta = 0$) and the stochastic case ($\sigma_\theta > 0$).

The proposed control schemes for the deterministic wind, which are based on analytic arguments, will give significant insights for the subsequent analysis and will illustrate some interesting patterns of the solution of the stochastic optimal control problem. It will be shown later on that the control strategies for each deterministic wind model, when applied to the DV in the presence of the stochastic wind, will capture the salient features of the solution of the stochastic optimal control problem.

## III. Feedback Laws with No Wind Information

In this section, feedback control laws are developed that drive the DV to its target in the presence of an unknown wind (W1). First, a method for designing a feedback control for the deterministic problem, that completely ignores the presence of a wind, is briefly discussed. Next, an optimal feedback control will be computed for the case where the Cartesian components of the wind vary stochastically. In all cases, the target set is a ball of radius with $\delta = 0.1$, and the velocity of the vehicle is constant $v = 1$.

### A. Deterministic Case

First, a control law that is completely independent of any information about the distribution of the wind is proposed. In other words, a feedback control law is designed under the assumption that

the wind is modeled by (W1) with $\sigma_W = 0$. Therefore, this control law is "blind" to the presence and the statistics of the actual wind. This approach will give two navigation laws that are similar to the pure pursuit strategy from missile guidance [20], which is a control strategy that forces the velocity vector of the controlled object (the DV in this case) to point towards its destination at every instant of time.

Note that in the presence of a wind and with the application of a feedback law that imitates the pure pursuit strategy, the DV will not be able to instantaneously change its motion in order to point its velocity vector toward the target. This happens for two reasons. The first reason is because the rate at which the DV can rotate its velocity vector is bounded by the turning rate constraint (3). The second reason has to do with the fact that, by hypothesis, the pure pursuit law does not account for the wind, and, consequently, even if the DV were able to rotate its forward velocity vector arbitrarily fast, it would be this forward velocity vector that points toward the target rather than the inertial velocity.

Let $\varphi$ be the angle between the vehicle's forward velocity vector and the line-of-sight to the target, given by $\varphi = \theta - \operatorname{atan}_2(y, x) + \pi$ and mapped to lie in $\varphi \in (-\pi, \pi]$ (see Fig. 1). The proposed (suboptimal) pure pursuit-like navigation law takes the following state-feedback form

$$u(\varphi) = \begin{cases} -1 & \text{if } \varphi \in (0, \pi], \\ 0 & \text{if } \varphi = 0, \\ +1 & \text{if } \varphi \in (-\pi, 0). \end{cases} \tag{5}$$

One important observation is that the control law (5) does not depend on the distance $r(t) = \sqrt{(x(t))^2 + (y(t))^2}$ of the DV from the target but only on the angle $\varphi$. The state feedback control law given in (5) will be referred to as the *geometric pure pursuit* (GPP for short) law. Note that the GPP law drives the DV to the line $\mathcal{S}_0 := \{(r, \varphi) : \ \varphi = 0\}$, which is a "switching surface." In the absence of wind, once the DV reaches $\mathcal{S}_0$, it travels along $\mathcal{S}_0$ until it reaches the target (such that $r = 0$ at the final time $T$) with the application of the control input $u = 0$. Therefore, the GPP law is a bang-off control law with one switching at most, that is, a control law which is necessarily a control sequence $\{\pm 1, 0\}$.

It is important to highlight that the GPP law turns out to be the time-optimal control law of

the MD problem for the majority (but not all) of the initial configurations $[x(0), y(0), \theta(0)]^\intercal$ (see Fig. 2), when there is no wind [21, 22]. However, there are still initial configurations from which the DV driven by the navigation law (5) either cannot reach the target set at all or can reach the target only suboptimally. The previous two cases are observed, for example, when the DV is close to the target with a relatively large $|\varphi|$.

[Fig. 2 about here.]

In particular, it can be shown [21, 22] that if the DV starts, at time $t = 0$, from any point that belongs to one of the two regions, $\mathcal{C}_+$ and $\mathcal{C}_-$, defined by (see Fig. 2)

$$\mathcal{C}_- = \{(r, \varphi) \ : \ r \leq 2\rho_{\min} \sin(-\varphi), \ \varphi < 0\} \tag{6}$$

$$\mathcal{C}_+ = \{(r, \varphi) \ : \ r \leq 2\rho_{\min} \sin(\varphi), \ \varphi > 0\}, \tag{7}$$

then the target cannot be reached by means of the GPP law in the absence of a stochastic wind (scenarios where the stochastic wind helps the DV to reach its target even by means of a GPP law will be shown later on). Therefore, in order to complete the design of a feedback control law for any possible state of the DV, one needs to consider the optimal solution of the MD problem in the case when the terminal heading is free [21, 22]. It turns out that the boundaries of $\mathcal{C}_+$ and $\mathcal{C}_-$, denoted, respectively, by $\mathcal{S}_-$ and $\mathcal{S}_+$ (the choice of the subscript notation will become apparent shortly later), correspond to two new "switching surfaces" along which the DV travels all the way to the target. In particular, when the DV starts in the interior of $\mathcal{C}_+$ (respectively, $\mathcal{C}_-$), then the minimum-time control action is $u = +1$ (respectively, $u = -1$), which may appear to be counterintuitive, since its effect is to increase $|\varphi|$ rather to decrease it. The control input remains constant until the DV reaches the "switching surface" $\mathcal{S}_-$ (respectively, $\mathcal{S}_+$), where the control switches to $u = -1$ (respectively, $u = +1$), and subsequently, the DV travels along $\mathcal{S}_-$ (respectively, $\mathcal{S}_+$) all the way to the target driven by $u = -1$ (respectively, $u = +1$). The net effect is that when the DV starts inside the regions $\mathcal{C}_\pm$, the DV must first distance itself from the target so that its minimum turning radius $\rho_{\min}$ is sufficient to turn towards the target. Note that in this case the control law is bang-bang with one switching at most, that is, a control sequence $\{\pm 1, \mp 1\}$. The situation is illustrated in Fig. 2 for $\rho_{\min} = 1$.

The GPP law given in (5), therefore, needs to be updated appropriately to account for the previous remarks. In particular, the new feedback control law is given by

$$u(r,\varphi) = \begin{cases} -1 & \text{if } (r,\phi) \in \Sigma_-, \\ 0 & \text{if } (r,\phi) \in \Sigma_0, \\ +1 & \text{if } (r,\phi) \in \Sigma_+, \end{cases} \tag{8}$$

where,

$$\Sigma_- := \{(r,\varphi) : \varphi \in (0,\pi]\} \cap (\text{int}\mathcal{C}_+)^c \cup \text{int}\mathcal{C}_-$$

$$\Sigma_+ := \{(r,\varphi) : \varphi \in (-\pi,0)\} \cap (\text{int}\mathcal{C}_-)^c \cup \text{int}\mathcal{C}_+$$

$$\Sigma_0 := \{(r,\varphi) : \varphi = 0\}.$$

The state feedback law (8) will be henceforth referred to as the *optimal pure pursuit* (OPP for short) law, because, at every instant of time, it steers the DV to the target based on the optimal strategy that corresponds to its current position. Note that in the absence of wind, the OPP law is the optimal control law of the MD problem with free final heading [21, 22]. One important remark about the OPP law is that the control variable $u$ may attain the value zero, which is in the interior of its admissible set $[-1,1]$. Thus, the control $u = 0$ is *singular*, and the part of the optimal trajectory it generates is referred to as the *singular arc* of the optimal solution. As explained in detail in Ref. [14], singular arcs may be part of the optimal solution of the MD problem in the absence of wind, only when the so-called *switching function* of the constrained optimal control problem, along with its first time derivative, vanish simultaneously (for a non-trivial time interval). Note that while $u = \pm 1$ corresponds to turning left/right, the control $u = 0$ corresponds to straight paths.

Figure 3 illustrates the level sets of the minimum time-to-go function, which can be computed analytically by using standard optimal control techniques and geometric tools, as shown in [14].

[Fig. 3 about here.]

### B. Stochastic Case

In this section, an optimal feedback control law for the stochastic kinematic model (W1) and cost functional (4) is developed. The optimal control is computed using the *Markov chain approximation*

*method* [17], which ensures that when discretizing a state space for value iteration in stochastic optimal control problems, the chosen spatial and temporal step sizes accurately scale in the same way as in the original stochastic process. The method constructs a discrete-time and discrete-state approximation to the cost function in the form of a controlled Markov chain that is "locally-consistent" with the process under control.

Since the method involves discretization of the state space, one first reduces the number of dimensions in the model (W1). Applying Itô's differentiation rule to the DV-target distance $r(t)$ and the viewing angle $\varphi(t)$ where $\varphi \in (-\pi, \pi]$, as before (see Fig. 1), it can be shown that the relative DV-target system coordinates obey (see the Appendix)

$$\mathrm{d}r(t) = \left(-v\cos(\varphi) + \frac{\sigma_W^2}{2r}\right)\mathrm{d}t + \sigma_W \mathrm{d}W_{\parallel}, \tag{9}$$

$$\mathrm{d}\varphi(t) = \left(\frac{v}{r}\sin(\varphi) + \frac{u}{\rho_{\min}}\right)\mathrm{d}t + \frac{\sigma_W}{r}\mathrm{d}W_{\perp}, \tag{10}$$

where $|u| \leq 1$, and where $\mathrm{d}W_{\parallel}$ and $\mathrm{d}W_{\perp}$ are mutually independent increments of unit intensity Wiener processes aligned with the direction of DV motion. Note the presence of a positive bias $\sigma_W^2/2r$ in the relation for $r(t)$, which is a consequence of the random process included in the analysis. In the proposed parametrization, only distances $r \geq \delta$ outside the target set are considered, and so (9)-(10) is well defined.

In the Appendix the equations for value iterations on the cost-to-go function using the Markov Chain approximation method are derived. From this, the optimal angular velocity of the DV may be obtained for any relative distance $r \geq \delta$ and viewing angle $\varphi$. The structure of the optimal control law (W1) is seen in Fig. 4(a) for $\sigma_W = 0.1$ and discretization steps $\Delta r = 0.02$ and $\Delta\phi = 0.025$. As in the deterministic model ($\sigma_W = 0$) case (Fig. 2), the value iteration stationary control law is composed of bang-bang regions instructing the DV to turn left or right and singular arcs. With smaller noise, the optimal control is comprised of four regions, two directing the target to turn left, and others instructing a turn to the right. The reader should note the similarity between Fig. 4(a) and the OPP control illustrated in Fig. 2. In particular, the structure of the regions $\mathcal{C}_-$ and $\mathcal{C}_+$ have changed somewhat, as a consequence of the stochastic variation of the wind. In Fig. 4(b), a higher noise intensity of $\sigma_W = 0.5$ causes the control to return to GPP control (5). In other words,

the variance of the process is so large that it becomes exceedingly difficult to predict the relative DV-target state, and the optimal control for the stochastic model matches a simpler, analytically-derived control for the deterministic model that, as described in the previous section, is not optimal for some initial conditions close to the target. This suggests that, for our problem, a deterministic control may suffice for the optimal feedback control when the variance of the stochastic wind is sufficiently large.

[Fig. 4 about here.]

This control strategy remains optimal for even larger $\sigma_W$, but due to the bias in $r(t)$ (see Eq. (9)), this control policy may not be successful in guiding the DV to the target in a reasonable amount of time for high values of $\sigma_W$. Although a solution to the backward Kolmogorov equation [19] indicates that the DV will eventually hit the target with probability one as $t \to \infty$, the expected value of the hitting time becomes exceedingly large with increasing $\sigma_W$. Similarly, one can also consider the probability that the DV, initially located at $(r, \varphi)$, will hit the target set by a specified time $\tau$ as a function of the noise intensity $\sigma_W$. Figure 5 shows this distribution as computed for $(r, \varphi) = (1, 0)$ and $\tau = 10\,\mathrm{s}$ using 1000 simulations for each $\sigma_W$.

[Fig. 5 about here.]

## IV. Feedback Laws for Wind at an Angle

Next, the second model (W2), in which the wind is now assumed to take on a direction $\theta_w$ with known speed $0 < v_w < 1$, where $v_w$ is constant by hypothesis, is assumed and the feedback control laws for steering the DV in the presence of this wind are discussed.

### A. Deterministic Case

First, the case when $\sigma_\theta = 0$ and $0 < v_w < 1$ is considered. Note that the fact that $\sigma_\theta = 0$ implies that the direction of the wind becomes constant, and consequently, the wind $w = [w_x,\ w_y]^\intercal$, where $w_x := v_w \cos\theta_w$ and $w_y := v_w \sin\theta_w$, is a constant vector. Therefore, in this section, it is

assumed that the constant wind $w$ is known a priori. The equations of motion of the DV become

$$\begin{aligned} \mathrm{d}x &= v\cos(\theta)\mathrm{d}t + w_x\mathrm{d}t, \\ \mathrm{d}y &= v\sin(\theta)\mathrm{d}t + w_y\mathrm{d}t, \\ \mathrm{d}\theta &= \frac{u}{\rho_{\min}}\mathrm{d}t, \qquad |u| \leq 1. \end{aligned} \tag{11}$$

First, a feedback law that is similar in spirit to the GPP law given in Eq. (5), which exploits the fact that the wind is known a priori, is designed. In particular, the proposed control law tries to rotate the velocity vector of the DV to point at the target. It is easy to show that the control law (5) becomes

$$u(\varphi) = \begin{cases} -1 & \text{if } \psi(\varphi) \in (0, \pi], \\ 0 & \text{if } \psi(\varphi) = 0, \\ +1 & \text{if } \psi(\varphi) \in (-\pi, 0). \end{cases} \tag{12}$$

and

$$\psi(\varphi) := \mathrm{atan}_2(\dot{y}, \dot{x}) - \theta + \varphi. \tag{13}$$

where $\psi$, is the angle between the inertial velocity of the DV and the line-of-sight (LOS) as is illustrated in Fig. 1 (the angle $\chi$ in this figure is equal to $\mathrm{atan}_2(\dot{y}, \dot{x})$). As it is shown in [20], the navigation law (12) is dual to the so-called *parallel navigation* law from missile guidance. The control law (12) is henceforth referred to as the Geometric Parallel Navigation (GPN for short) law.

As mentioned in Section III A, the GPP law that forces the forward velocity of the vehicle to point towards the target may not always be well defined, especially in the vicinity of the target. The same type of argument applies to the GPN law modulo the replacement of the forward velocity with the inertial velocity. Next, a control law that steers the DV to the target using the optimal control that correspond to the current position of the DV and assuming a constant (e.g., average) wind is presented. This control law is referred to as the Optimal Parallel Navigation (OPN for short) law. Note that similarly to the GPN law, the OPN law does not consider the variations of both the speed and the direction of the wind. By combining the type of arguments used in [21, 22], which deal with the standard MD problem with free terminal heading, along with the analysis presented

in [11, 12], one can easily show that the candidate optimal control of the Markov-Dubins problem in the presence of a constant wind corresponds to the four control sequences presented in Section III A, namely, $\{\pm 1, 0\}$ and $\{\pm 1, \mp 1\}$. The main difference between the solutions of the Markov-Dubins problem in the absence of a wind, which was briefly presented in Section III A, and the Markov-Dubins problem in the presence of a constant wind, is the switching conditions and, consequently, the switching times of their common control sequences.

[Fig. 6 about here.]

Figure 6 illustrates the structure of the OPN law in the $(r, \varphi)$ plane in the presence of a constant tailwind, that is, $\theta_w = \theta(0)$, and a constant headwind, that is, $\theta_w = \pi + \theta(0)$, respectively. One observes that the GPN law coincides with the OPN law for the majority of the boundary conditions especially for the case of a tailwind, whereas in the presence of the headwind the points in the $(r, \varphi)$ plane where the optimal strategy is bang-bang correspond to a significantly large set. An interesting observation is that the new switching surfaces of the OPN law are associated with those of the OPP law by means of a particular coordinate transformation $\mathcal{H} : (x, y, \theta) \mapsto (x', y', \theta)$, as described in [12]. In particular, a configuration with coordinates $(x, y, \theta)$ that belongs to the switching surface $\mathcal{S}_+$, $\mathcal{S}_0$ or $\mathcal{S}_-$ of the OPP law corresponds to a point with coordinates $(x', y', \theta)$ that belongs respectively to the switching surface $\mathcal{S}_+$, $\mathcal{S}_0$ and $\mathcal{S}_-$ of the OPN law, where

$$x' = x + w_x T_{\mathrm{DV}}(x, y, \theta), \tag{14}$$

$$y' = y + w_y T_{\mathrm{DV}}(x, y, \theta), \tag{15}$$

where $T_{\mathrm{DV}}(x, y, \theta)$ is the minimum time required to drive the DV from $(x, y, \theta)$ to the origin with free final heading $\theta$. It is easy to show that for a state $(x, y, \theta) \in \mathcal{S}_+$ $(\mathcal{S}_-)$, it holds that $T_{\mathrm{DV}}(x, y, \theta) = -2\rho_{\min}\varphi(x, y, \theta)/v$ $(2\rho_{\min}\varphi(x, y, \theta)/v)$. In addition, if the state $(x, y, \theta) \in \mathcal{S}_0$, then $T_{\mathrm{DV}}(x, y, \theta) = \sqrt{x^2 + y^2}/v$.

Figure 7 illustrates the correspondence of the switching surfaces of the OPN law with those of the OPP law for a tailwind $(\theta_w = \theta(0) = 0)$ and a headwind $(\theta_w = \pi + \theta(0) = \pi)$ via the previous coordinate transformation. Note that the switching surface $\mathcal{S}_0$ of both the OPG and the OPP laws are the same but the surfaces $\mathcal{S}_\pm$ are different.

[Fig. 7 about here.]

Figure 8 illustrates the level sets of the minimum time-to-go function in the presence of a constant wind, whose computation entails the solution of a decoupled system of transcendental equations as shown in [11, 12]. In particular, Fig. 8(a) and Fig. 8(b) illustrate the level sets of the minimum time-to-go function in the presence of a constant tailwind and a constant headwind, respectively.

[Fig. 8 about here.]

### B. Stochastic Case

It is now assumed that the direction of the wind $\theta_w$ is no longer constant, but is rather described by the stochastic process (W2) with $\sigma_\theta > 0$. A similar derivation to that used for model (W1) yields for (W2):

$$\begin{aligned} \mathrm{d}r(t) &= -\left(v\cos(\varphi) + v_w\cos(\varphi+\gamma)\right)\mathrm{d}t, \\ \mathrm{d}\varphi(t) &= \left(\frac{v}{r}\sin(\varphi) + \frac{v_w}{r}\sin(\varphi+\gamma) + \frac{u}{\rho_{\min}}\right)\mathrm{d}t, \\ \mathrm{d}\gamma(t) &= \frac{u}{\rho_{\min}}\mathrm{d}t - \sigma_\theta \mathrm{d}W_\theta, \end{aligned} \tag{16}$$

where the state $\gamma(t) := \theta(t) - \theta_w(t)$ is introduced to define the difference between the DV heading angle and the direction of the wind $\theta_w$. In the numerical example, the following data are used: $v_w = 0.5$, and $\sigma_\theta = 0.1$. The discretization steps were chosen as $\Delta r = 0.1$, $\Delta\phi = 0.08$, and $\Delta\gamma = 0.12$. As before, value iterations on the optimal cost-to-go were performed as described in the Appendix. Two "slices" of this control, corresponding to the cases where the DV travels in the direction of the wind (tailwind, where $\gamma = 0$) and where it faces the wind (headwind, $\gamma = \pi$) are shown in Figs. 9(a) and 9(b), respectively. In each fixed-$\gamma$ policy, the optimal control resembles that shown in Fig. 6, although the location and shape of the switching curves $\mathcal{S}_\pm$ have changed due to the stochastic variation in the wind. In Fig. 9(a), only small vestiges of the switching curves are seen, while in Fig. 9(b), the shape of these curves has changed. Figure 10 shows the expected value of the time required to hit the target in the case of a headwind and tailwind.

[Fig. 9 about here.]

[Fig. 10 about here.]

## V. Performance Comparison

In the previous sections, it is seen that the control laws for both deterministic wind models closely resemble their respective optimal feedback control laws for the stochastic wind models. In particular, the control policies for the deterministic and stochastic wind models are identical when far from the target, but differences are seen when $r$ is close to $\delta$. To see the effect of these differences, this section provides a comparison of performance of the proposed feedback control laws against the stochastic wind models (W1) and (W2).

[Fig. 11 about here.]

As an example, Fig. 11 shows a collection of simulated DV trajectories under the controls for the deterministic (red) and stochastic (blue or green) wind models, where the left and right panels correspond to (W1) and (W2), respectively. In this figure, the control anticipating the wind stochasticity assumes that there is a non-zero probability that the stochastic wind may push it beyond its minimum turning radius $\rho_{\min}$ and into the target, and hence the control directs it to perform a left turn. Some realizations (75.6%, shown in green) under this control reach the target, but the remainder (blue) must circle around (see insert). The control for the deterministic wind model directs the red DVs to first distance themselves before approaching the target. Consequently, the regions in the $(r, \varphi)$ state space corresponding to the trajectories in this example lead to a smaller expected time to hit the target for the stochastic model-based control, as seen in Fig. 12. However, there is also a chance that the stochastic model-based control is unsuccessful in hitting the target on its first pass, and so the DV must circle around again. In other words, the stochastic model-based control "risks" a turn toward the target for small $r$ and small $\varphi$. Although the expected value of the hitting time decreases under the control anticipating the stochastic winds, the standard deviation of these times may simultaneously increase, as seen in Fig 12.

[Fig. 12 about here.]

In the right panel of Fig. 11, a similar result is seen for the case of wind at an angle (indicated by a $v_w$ arrow). In this case, a small number of the realizations for the DVs under the deterministic model-based control are affected by the changing wind and must take a longer route to reach the target, whereas the DVs under the stochastic model-based control anticipate the changing wind direction. Similarly, Fig. 13 shows the mean time-to-go under (W2) using both the control for the deterministic model shown in Fig. 6 and the control law for the stochastic wind model in Fig. 9. As before, the expected time-to-go is larger for the deterministic model-based control in regions where the control laws differ. However, unlike (W1), the standard deviation under the stochastic model-based control was consistently smaller since the control accounts for the stochastic wind without instructing for a potentially "risky" approach to the target.

[Fig. 13 about here.]

## VI. Conclusions and Future Work

In this paper, the problem of guiding a vehicle with Dubins-type kinematics to a prescribed target set with free final heading in the presence of a stochastic wind in minimum expected time has been addressed. Two approaches to this problem have been proposed. The first one, which was based on analytic techniques, was to employ feedback control laws, based on a deterministic model, that are similar to the well-studied pure pursuit and the parallel navigation laws from the field of missile guidance. The proposed feedback control laws are time-optimal in the absence of wind or in the presence of a wind that is constant and known a priori.

The second approach was to tackle the problem computationally by employing numerical tools from stochastic optimal control theory. Because these control laws are based explicitly on the stochastic wind models, they anticipate the wind stochasticity, and the time necessary to steer the Dubins vehicle to the target set in the presence of a stochastic wind is, on average, lower than that under the control for the corresponding deterministic model. However, although the feedback control laws for the deterministic model become suboptimal in the presence of a stochastic wind, it turns out that they still manage to steer the Dubins vehicle to its target set with an acceptable miss target error. On the other hand, a stochastic framework leads to higher expected precision in

terms of target miss-distance and more predictable trajectories.

The fact that the deterministic model-based controls perform so well for this problem even in the presence of an unknown stochastic wind is mainly owing to the fact that they are in a feedback form, thus providing a certain degree of robustness against uncertainties. Having that in mind, it may not be surprising that the presented deterministic model-based control laws can work in the presence of small stochastic disturbances, although non-optimally. This may not be the case for other problems in practice where one is only able to generate reliable deterministic *open-loop* trajectories. Surprisingly perhaps, the computation of optimal feedback controls based on *stochastic* models generally is no more difficult (or even easier) than for their deterministic counterparts as the latter can be consistently discretized and cast as a controlled Markov decision process, as shown in this paper. On the other hand, the closed-form feedback laws based on the deterministic model presented in this paper may be more appealing than their stochastic model-based counterparts, owing to their ease of implementation.

Thus, the similarity between control policies under different levels of wind stochasticity seems to support the use of the feedback controls for deterministic wind models in lieu of stochastic model-based feedback controls when the stochastic effects are small, or can be used as "seeds" that may expedite the computation of the solution to the stochastic optimal control problem, or aid in the verification of numerical results. Moreover, since the role of noise in designing feedback control policies is not fully understood, a side-by-side comparison of the feedback laws for deterministic and stochastic models in other problems may provide useful insights toward a more general theory.

Future work will include the extension of the techniques presented herein to problems with a more realistic model of the wind, including wind models that depend explicitly on the position of the Dubins vehicle. Another possible extension is to characterize control laws for stochastic wind models that minimize a cost function taking into consideration both the expected value and the variance of the time-to-go.

## Appendix

### Derivation of Relative Stochastic Kinematic Model (9)-(10) for (W1)

Given a stochastic differential equation for the state $\mathbf{x} \in \mathbb{R}^n$ in the form

$$\mathrm{d}\mathbf{x}(t) = b(\mathbf{x})\mathrm{d}t + a(\mathbf{x})\mathrm{d}W(t),$$

the Itô Lemma states that the total differential of a scalar, time-independent function $f(\mathbf{x})$ is

$$\mathrm{d}\left[f(\mathbf{x})\right](t) = \left(b(\mathbf{x})\mathrm{d}t + a(\mathbf{x})\mathrm{d}W(t)\right)^{\intercal} \nabla_{\mathbf{x}} f(\mathbf{x}) + \frac{1}{2}\left(a(\mathbf{x})\mathrm{d}W(t)\right)^{\intercal} \nabla^2_{\mathbf{x}} f(\mathbf{x}) \left(a(\mathbf{x})\mathrm{d}W(t)\right),$$

where, if $\mathrm{d}W(t)$ is of dimension $k$, we also have by definition that $\mathrm{d}W^{\intercal}\mathrm{d}W = I_{k\times k}\mathrm{d}t$. Applying this rule to (W1), we may obtain the total differential for $r(t) = \sqrt{(x(t))^2 + (y(t))^2}$ as

$$\begin{aligned}
\mathrm{d}r(t) &= \frac{x}{r}\mathrm{d}x(t) + \frac{y}{r}\mathrm{d}y(t) + \frac{1}{2}\left(\frac{1}{r} - \frac{x^2}{r^3}\right)(\mathrm{d}x(t))^2 + \frac{1}{2}\left(\frac{1}{r} - \frac{y^2}{r^3}\right)(\mathrm{d}y(t))^2 - \frac{xy}{r^3}(\mathrm{d}x(t))(\mathrm{d}y(t)) \\
&= \left(-v\cos(\varphi) + \frac{\sigma_W^2}{2r}\right)\mathrm{d}t - \sigma_W\cos(\theta-\varphi)\mathrm{d}W_x - \sigma_W\sin(\theta-\varphi)\mathrm{d}W_y, \qquad (17)
\end{aligned}$$

where we have used the fact that $x/r = -\cos(\theta-\varphi)$ and $y/r = -\sin(\theta-\varphi)$. Similarly, since $\tan^{-1}(y/x) = \theta - \varphi + \pi$, the total differential for $\varphi$ is

$$\begin{aligned}
\mathrm{d}\varphi(t) &= \frac{u}{\rho_{\min}}\mathrm{d}t + \frac{y}{r^2}\mathrm{d}x(t) - \frac{x}{r^2}\mathrm{d}y(t) - \frac{xy}{r^4}(\mathrm{d}x(t))^2 + \frac{xy}{r^4}(\mathrm{d}y(t))^2 \\
&= \left(\frac{v}{r}\sin\varphi + \frac{u}{\rho_{\min}}\right)\mathrm{d}t + \frac{\sigma_W}{r}\sin(\theta-\varphi)\mathrm{d}W_x - \frac{\sigma_W}{r}\cos(\theta-\varphi)\mathrm{d}W_y. \qquad (18)
\end{aligned}$$

Since the components of the original 2D Brownian motion model are scaled with the same parameter $\sigma_W$, the noise is invariant under a rotation of the coordinate frame [19]. Defining $\mathrm{d}W_{\parallel}(t)$ and $\mathrm{d}W_{\perp}(t)$ as the increments $\mathrm{d}W_x$ and $\mathrm{d}W_y$ when viewed in a coordinate frame aligned with the direction of DV motion, we obtain (9)-(10).

### Derivation of Value Iteration Equations

The following derivation of the equations for value iteration is specific to the wind model (W2). The discretization details for (W1) may be found in [15]. Denote by $\mathcal{L}^u$ the differential operator associated with the stochastic process (16), which, for the sake of brevity, one writes in terms of the mean drift $\mathbf{b}(\mathbf{x}, u) \in \mathbb{R}^3$, the diffusion $\mathbf{a}(\mathbf{x}) \in \mathbb{R}^{3\times 3}$ and the state vector $\mathbf{x} = [r, \varphi, \gamma]^{\intercal}$, as follows

$$\mathrm{d}\mathbf{x} = b(\mathbf{x}, u)\mathrm{d}t + a(\mathbf{x})\mathrm{d}W(t)$$

with the associated differential operator

$$\mathcal{L}^u = \sum_{i=1}^{3} b_i(\mathbf{x}, u)\frac{\partial}{\partial x_i} + \frac{1}{2}\sum_{i,j=1}^{3} a_{ij}(\mathbf{x})\frac{\partial^2}{\partial x_i \partial x_j}.$$

The state $\mathbf{x}$ is in the domain $\mathbb{X} = \{\mathbf{x} \mid \delta \leq r < r_{\max}, -\pi \leq \varphi \leq \pi, -\pi \leq \gamma \leq \pi\}$, which is semi-periodic because $[r,\ \pi, \gamma]^\intercal = [r, -\pi, \gamma]^\intercal$ and $[r,\ \varphi, -\pi]^\intercal = [r, \varphi, \pi]^\intercal$. It follows that the domain boundary is composed of two disjoint segments, i.e., $\partial\mathbb{X} = \{\mathbf{x}\ :\ r = \delta\} \cup \{\mathbf{x}\ :\ r = r_{\max}\}$.

It can be shown [17] that a sufficiently smooth $J(\mathbf{x})$ given by (4) satisfies

$$\mathcal{L}^u J(\mathbf{x}) + 1 = 0, \tag{19}$$

so that the stochastic Hamilton-Jacobi-Bellman equation for the minimum cost $V(\mathbf{x})$ over all control sequences is

$$\inf_{|u|\leq 1} [\mathcal{L}^u V(\mathbf{x}) + 1] = 0. \tag{20}$$

This PDE has mixed boundary conditions on $\partial\mathbb{X}$. At $r = r_{\max}$, one can use reflecting boundary conditions $(\nabla V(\mathbf{x}))^\intercal \hat{n} = 0$ with the boundary normals $\hat{n}$. For the part of boundary $r = \delta$ that belongs to the target set $\mathcal{T}$, one has to use an absorbing boundary condition with $V(\mathbf{x}) = g(\mathbf{x}) \equiv 0$.

A discrete-time Markov chain $\{\xi_n, n < \infty\}$ with controlled transition probabilities from the state $\mathbf{x}$ to the state $\mathbf{y} \in \mathbb{X}$ denoted by $p(\mathbf{y} \mid \mathbf{x}, u)$ is introduced. A continuous-time approximation $\xi(t)$ to the original process $\mathbf{x}(t)$ is created by way of a state- and control-dependent interpolation interval $\Delta t_u = \Delta t(\mathbf{x}, u) = t_{n+1} - t_n$ via $\xi(t) = \xi_n$ where $t \in [t_n, t_{n+1})$ [17]. The transition probabilities $p(\mathbf{y} \mid \mathbf{x}, u)$ then appear as coefficients in the finite-difference approximations of the operator $\mathcal{L}^u$ in (19). Using the so-called up-wind approximations for derivatives, the finite-difference discretizations for $J(\cdot)$ with step sizes $\Delta r$, $\Delta\varphi$, and $\Delta\gamma$ are

$$\begin{aligned} J^h(r,\varphi,\gamma) = \Delta t^u + \sum_{i=1,2} \Big\{ & p\left(r - (-1)^i\Delta r, \varphi, \gamma \mid r, \varphi, \gamma, u\right) J^h(r - (-1)^i\Delta r, \varphi, \gamma) \\ & + p\left(r, \varphi - (-1)^i\Delta\varphi, \gamma \mid r, \varphi, \gamma, u\right) J^h(r, \varphi - (-1)^i\Delta\varphi, \gamma) \\ & + p\left(r, \varphi, \gamma - (-1)^i\Delta\gamma, \mid r, \varphi, \gamma, u\right) J^h(r, \varphi, \gamma - (-1)^i\Delta\gamma) \Big\} \end{aligned} \tag{21}$$

where the coefficients multiplying $J^h(\cdot)$ are the respective transition probabilities, given by

$$
\begin{aligned}
p\left(r \pm \Delta r, \varphi, \gamma \mid r, \varphi, \gamma, u\right) &= \Delta t^u \frac{\max\left[0, \left(\mp v\cos(\varphi) \mp v_w \cos\left(\varphi+\gamma\right)\right)\right]}{\Delta r}, \\
p\left(r, \varphi \pm \Delta\varphi, \gamma \mid r, \varphi, \gamma, u\right) &= \Delta t^u \frac{\max\left[0, \left(\pm(v/r)\sin(\varphi) \pm (v_w/r)\sin\left(\varphi+\gamma\right) \pm u/\rho_{\min}\right)\right]}{\Delta\varphi}, \\
p\left(r, \varphi, \gamma \pm \Delta\gamma \mid r, \varphi, \gamma, u\right) &= \Delta t^u \left(\frac{\max\left[\left(\pm u/\rho_{\min}\right)\right]}{\Delta\gamma} + \frac{\sigma_\theta^2}{2(\Delta\gamma)^2}\right),
\end{aligned} \tag{22}
$$

where "max" is a result of the up-wind approximation, and where $\Delta t^u$, given by

$$
\begin{aligned}
\Delta t^u(\mathbf{x}) = \Bigg(&\frac{\left|-v\cos(\varphi) - v_w\cos\left(\varphi+\gamma\right)\right|}{\Delta r} + \frac{\left|(v/r)\sin\left(\varphi+\gamma\right) + (v_w/r)\sin\left(\varphi+\gamma\right) + u/\rho_{\min}\right|}{\Delta\varphi} \\
&+ \frac{|u/\rho_{\min}|}{\Delta\gamma} + \frac{\sigma_\theta^2}{(\Delta\gamma)^2}\Bigg)^{-1},
\end{aligned}
$$

ensures that all probabilities sum to unity.

The Markov chain defined by these transition probabilities satisfies the requirement of "local consistency," in the sense that the drift and covariance of the Markov process $\xi(t)$ are consistent with the drift and covariance of the original process, and the cost-to-go $V^h(\cdot)$ for $\xi(t)$, therefore, suitably approximates that associated with the original process. The dynamic programming equation for the Markov chain used for value iteration, is given as follows [17]:

$$
V^h(\mathbf{x}) = \min_{|u|\le 1}\left\{\Delta t^u(\mathbf{x}, u) + \sum_{\mathbf{y}} p(\mathbf{y} \mid \mathbf{x}, u) V^h(\mathbf{y})\right\}, \tag{23}
$$

for all $\mathbf{x} \in \mathbb{X} \setminus \partial\mathbb{X}$. For the reflective part of the boundary, $r = r_{\max}$ (see Ref. [17, pp. 143]) is used instead of (23):

$$
V^h(\mathbf{x}) = \sum_{\mathbf{y}} p(\mathbf{y} \mid \mathbf{x}) V^h(\mathbf{y}), \tag{24}
$$

where $p(\mathbf{y} \mid \mathbf{x}) = 1$ for $\mathbf{y} = [r_{\max} - \Delta r, \varphi, \gamma]^\intercal$ and $\mathbf{x} = [r_{\max}, \varphi, \gamma]^\intercal$; otherwise, $p(\mathbf{y} \mid \mathbf{x}) = 0$. Finally, for those states $\mathbf{x} \in \mathcal{T}$ in the target set, it is imposed that

$$
V^h(\mathbf{x}) = 0. \tag{25}
$$

Equations (23)-(25) are used in the method of value iteration until the cost converges. From this, given the wind speed $v_w$, one obtains the optimal angular velocity of the DV for any relative distance $r$, viewing angle $\varphi$, and relative wind direction $\gamma$.

**Acknowledgments**

The authors wish to thank the reviewers for their comments and thoughtful insight. This work was supported by the NSF GRFP 0809125.

**References**

[1] Dubins, L. E., "On curves of minimal length with a constraint on average curvature, and with prescribed initial and terminal positions and tangents," *American Journal of Mathematics*, Vol. 79, No. 3, 1957, pp. 497–516.

[2] Isaacs, R., "Games of pursuit," RAND Report P-257, RAND Corporation, Santa Monica, CA, 1951.

[3] Patsko, V. S. and Turova, V. L., "Numerical study of the "homicidal chauffeur" differential game with the reinforced pursuer," *Game Theory and Applications*, Vol. 12, 2007, pp. 123–152.

[4] Sussmann, H. J., "The Markov-Dubins problem with angular acceleration control," *Proceedings of 36th IEEE Conference on Decision and Control*, San Diego, CA, Dec. 1997, pp. 2639–2643.

[5] Rysdyk, R., "Unmanned aerial vehicle path following for target observation in wind," *Journal of Guidance, Control, and Dynamics*, Vol. 29, No. 5, 2006, pp. 1092–1100, doi: 10.2514/1.19101.

[6] Ceccarelli, N., Enright, J. J., Frazzoli, E., Rasmussen, S. J., and Schumacher, C. J., "Micro UAV path planning for reconnaisance in wind," *Proceedings of American Control Conference*, New York City, NY, July 11–13, 2007, pp. 5310–5315.

[7] Nelson, D. R., Barber, D. B., McLain, T. W., and Beard, R. W., "Vector Field Path Following for Miniature Air Vehicles," *IEEE Transanctios on Robotics and Automation*, Vol. 23, No. 3, 2007, pp. 519–529, doi: 10.1109/TRO.2007.898976.

[8] Zhu, S., Wang, D., and Chen, Q., "Standoff tracking control of moving target in unknown wind," *Proceedings of the 48th IEEE Conference on Decision and Control*, Shanghai, China, December 15–18, 2009, pp. 776–781.

[9] McGee, T. G. and Hedrick, J. K., "Optimal path planning with a kinematic airplane model," *Journal of Guidance, Control, and Dynamics*, Vol. 30, No. 2, 2007, pp. 629–633, doi: 10.2514/1.25042.

[10] Techy, L. and Woolsey, C. A., "Minimum-time path-planning for unmanned aerial vehicles in steady uniform winds," *Journal of Guidance, Control, and Dynamics*, Vol. 32, No. 6, 2009, pp. 1736–1746, doi: 10.2514/1.44580.

[11] Bakolas, E. and Tsiotras, P., "Time-optimal synthesis for the Zermelo-Markov-Dubins problem: the constant wind case," *Proceedings of American Control Conference*, Baltimore, MD, June 30–July 2, 2010, pp. 6163–6168.

[12] Bakolas, E., *Optimal steering for kinematic vehicles with applications to spatially distributed agents*, Ph.D. dissertation, School of Aerospace Engineering, Georgia Institute of Technology, Atlanta, GA, 2011.

[13] McNeely, R. L., Iyer, R. V., and Chandler, P. R., "Tour planning for an unmanned air vehicle under wind conditions," *Journal of Guidance, Control, and Dynamics*, Vol. 30, No. 5, 2007, pp. 1299–1306, doi: 10.2514/1.26055.

[14] Bakolas, E. and Tsiotras, P., "Optimal Synthesis of the asymmetric sinistral/dextral Markov-Dubins problem," *Journal of Optimization Theory and Applications*, Vol. 150, No. 2, 2011, pp. 233–250, doi: 10.1007/s10957-011-9841-3.

[15] Anderson, R. P. and Milutinović, D., "Dubins vehicle tracking of a target with unpredictable trajectory," *in Proc. 4th ASME Dynamic Systems and Control Conference*, Arlington, VA, Oct. 31–Nov. 2, 2011.

[16] Anderson, R. P. and Milutinović, D., "A Stochastic Approach to Dubins Feedback Control for Target Tracking," *IEEE/RSJ International Conference on Intelligent Robots and Systems*, San Francisco, CA, Sep. 25–30, 2011, pp. 3917–3922.

[17] Kushner, H. J. and Dupuis, P., *Numerical Methods for Stochastic Control Problems in Continuous Time*, Springer, 2nd ed., 2001, Chaps. 3–5, pp. 53–151.

[18] Bertsekas, D. P. and Tsitsiklis, J. N., *Neuro-Dynamic Programming*, Athena Scientific, Belmont, MA, 1996, Chap. 2, pp. 12–57.

[19] Gardiner, C., *Stochastic Methods: A Handbook for the Natural and Social Sciences*, Springer, 4th ed., 2009, Chaps. 1–4., pp. 1–116.

[20] Bakolas, E. and Tsiotras, P., "Feedback Navigation in an Uncertain Flow-Field and Connections with Pursuit Strategies," *Journal of Guidance, Control, and Dynamics*, Vol. 35, No. 4, 2012, pp. 1268–1279, doi: 10.2514/1.54950.

[21] Boissonnat, J. D. and Bui, X. N., "Accessibility region for a car that only moves forward along optimal paths," Research Note 2181, Institut National de Recherche en Informatique et en Automatique, Sophia-Antipolis, France, 1994.

[22] Thomaschewski, B., "Dubins' problem for the free terminal direction," *Preprint*, 2001, pp. 1–14.

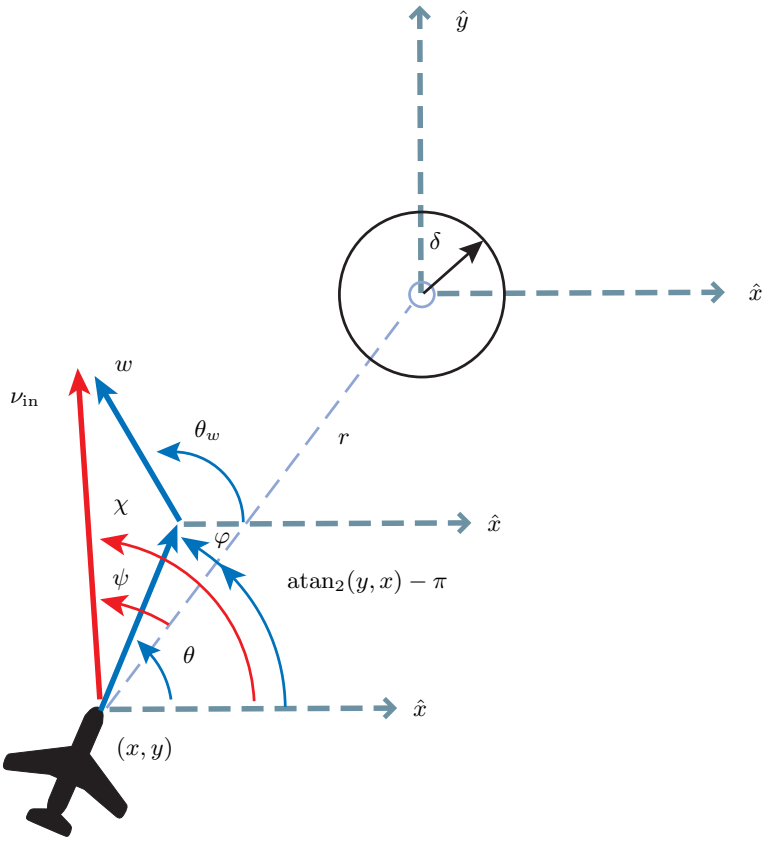


**Fig. 1 Diagram of a DV at position $[x(t),\ y(t)]^\intercal$ moving at heading angle $\theta$ in order to converge on a target in minimum time in the presence of wind. The target set $\mathcal{T}$ is shown as a circle of radius $\delta$ around the target. In the presence of the wind vector $w$ at an angle $\theta_w$, the DV travels in the direction of its inertial velocity vector $\nu_{\text{in}}$ and with a line-of-sight angle $\varphi$ to the target center. The angle between $\nu_{\text{in}}$ and the line-of-sight angle is $\varphi$, and $\chi$ is the angle $\text{atan}_2(\dot{y}, \dot{x})$.**

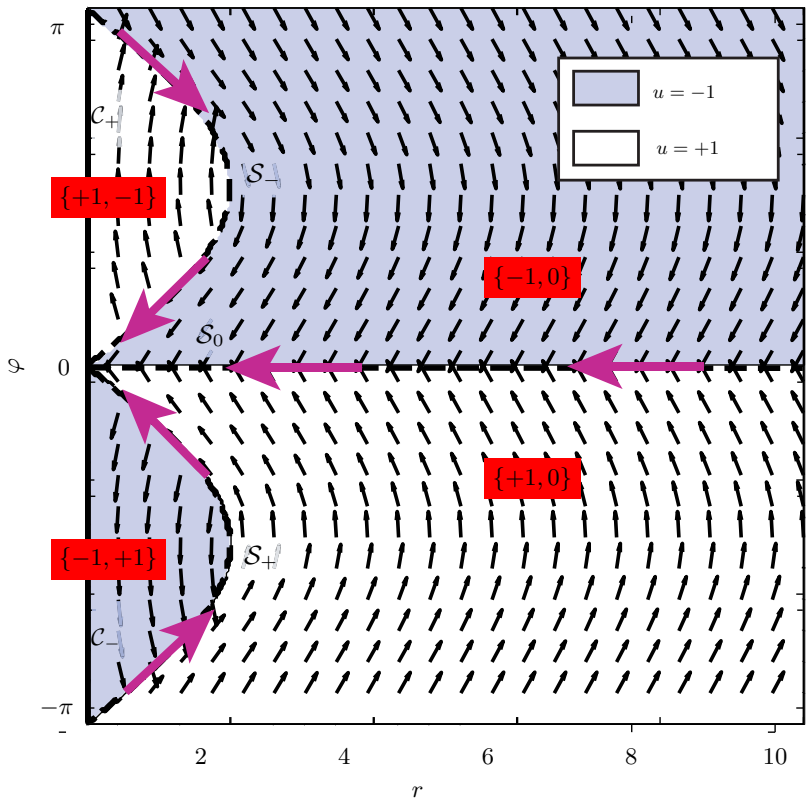


**Fig. 2 Time-optimal partition of the control input space and state feedback control law of the MD problem with free terminal heading in the absence of wind. One can use this control strategy as a feedback law for the case of a stochastic wind. Control sequences for an initial state in each time-optimal partition are indicated in red background.**

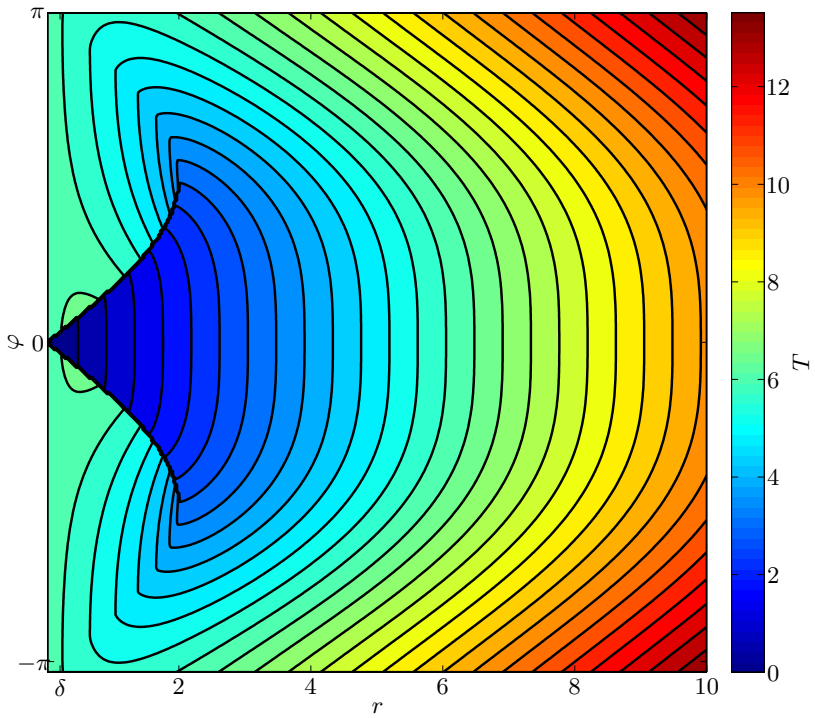


**Fig. 3 Level sets of the minimum time-to-go function of the MD problem with free terminal heading.**

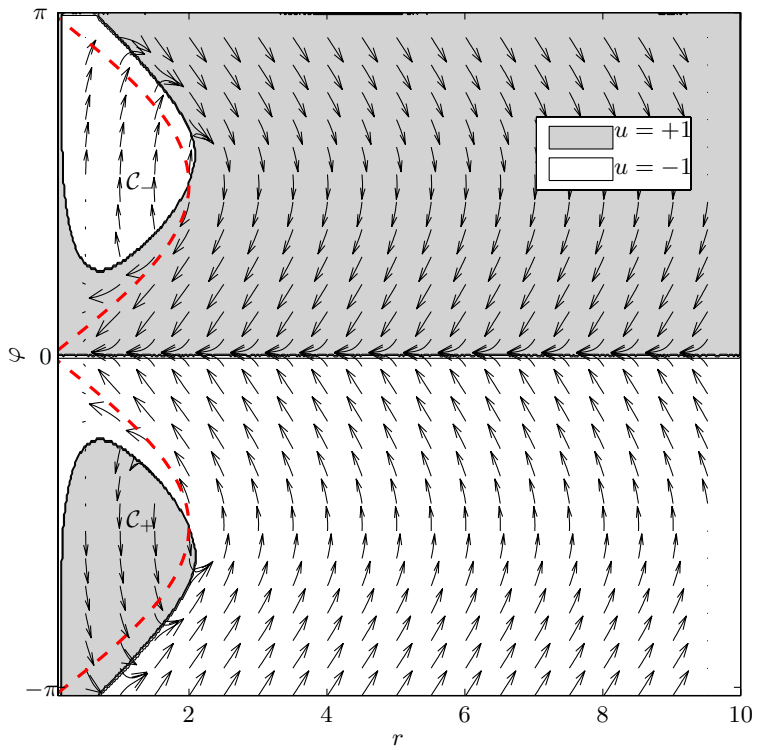


(a) Stochastic optimal control policy for $\sigma_W = 0.1$. For comparison, the switching curves from the deterministic model-based OPP control in Fig. 2 are outlined in red.

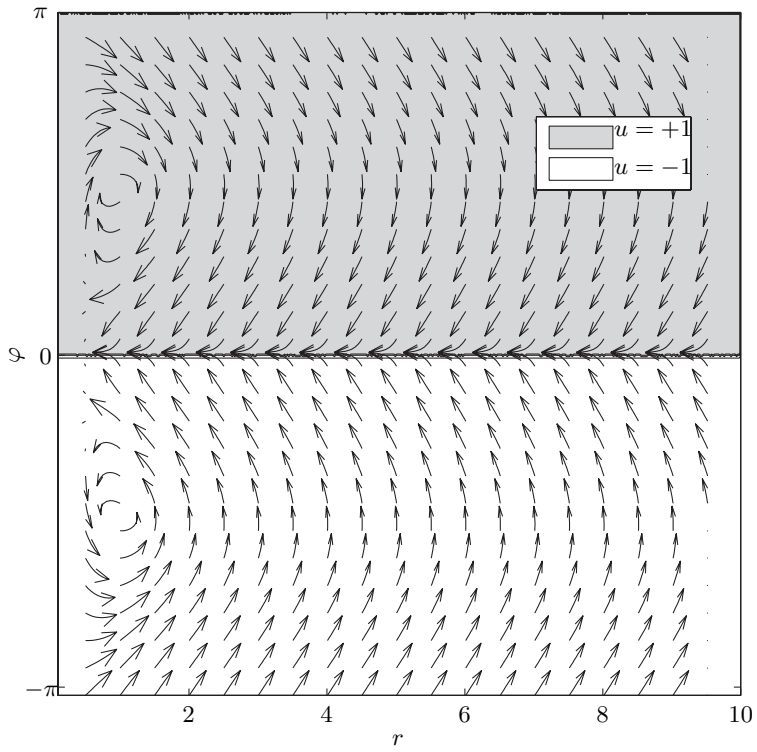


(b) Stochastic optimal control policy for $\sigma_W = 0.5$ yields the GPP control (5) for deterministic winds.

**Fig. 4 Dubins vehicle optimal turning rate control policy $u(r, \varphi)$ for model (W1).**

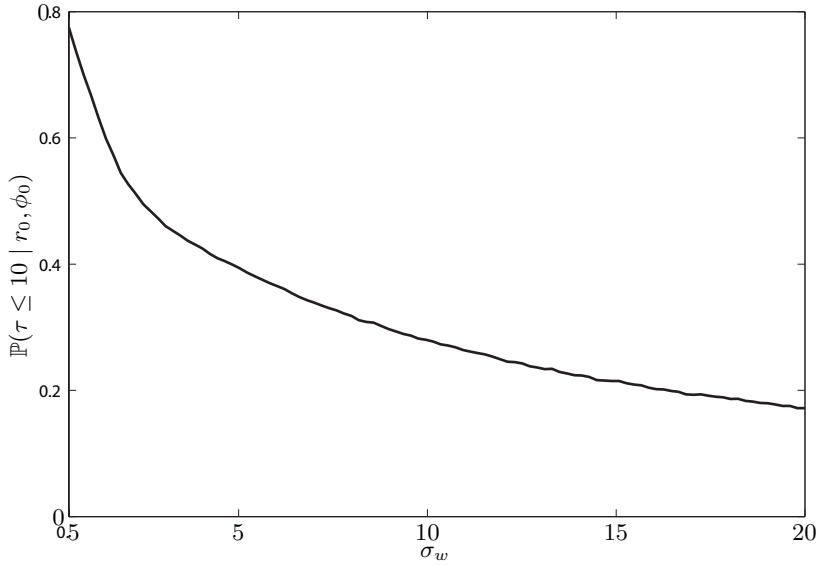


**Fig. 5 Probability of hitting the target set in the time interval $0 < \tau \leq 10$ for an initial condition a distance 1 [m] from the target and facing towards the target ($(r, \varphi) = (1, 0)$).**

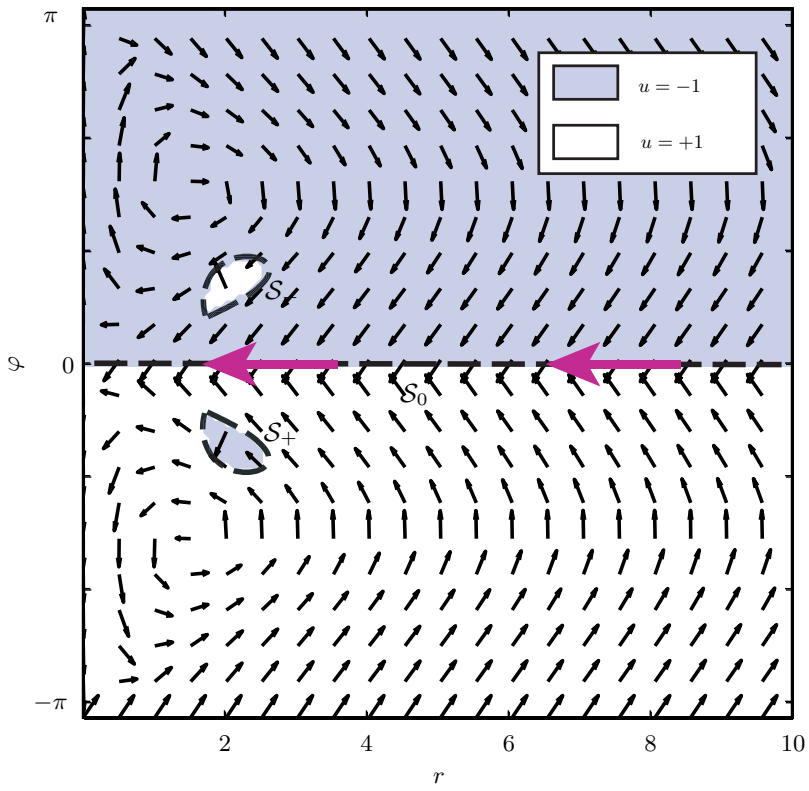


(a) Tailwind.

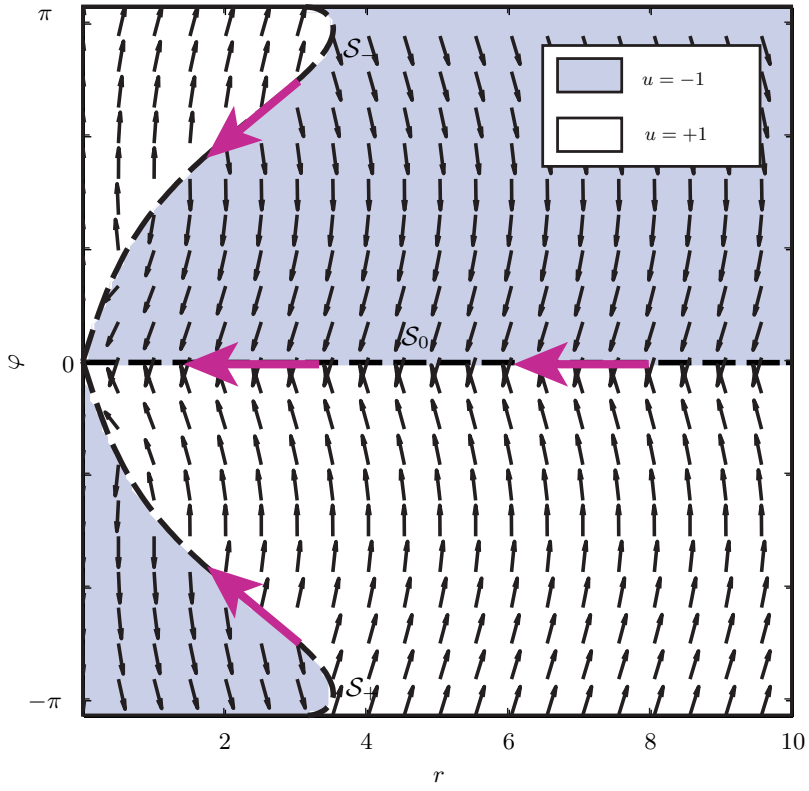


(b) Headwind.

**Fig. 6 Time-optimal partition of the control input space and state feedback control law of the MD problem with free terminal heading in the presence of a constant wind.**

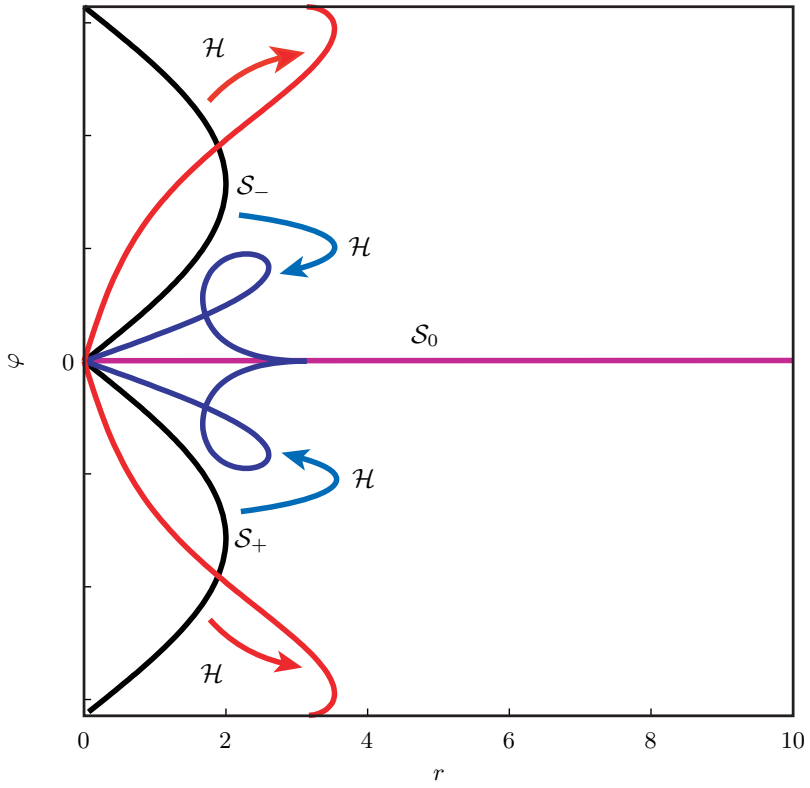


**Fig. 7 Correspondence between the switching surfaces of the OPP and the OPG laws via a transformation for a tailwind (blue curves) and a headwind (red curves).**

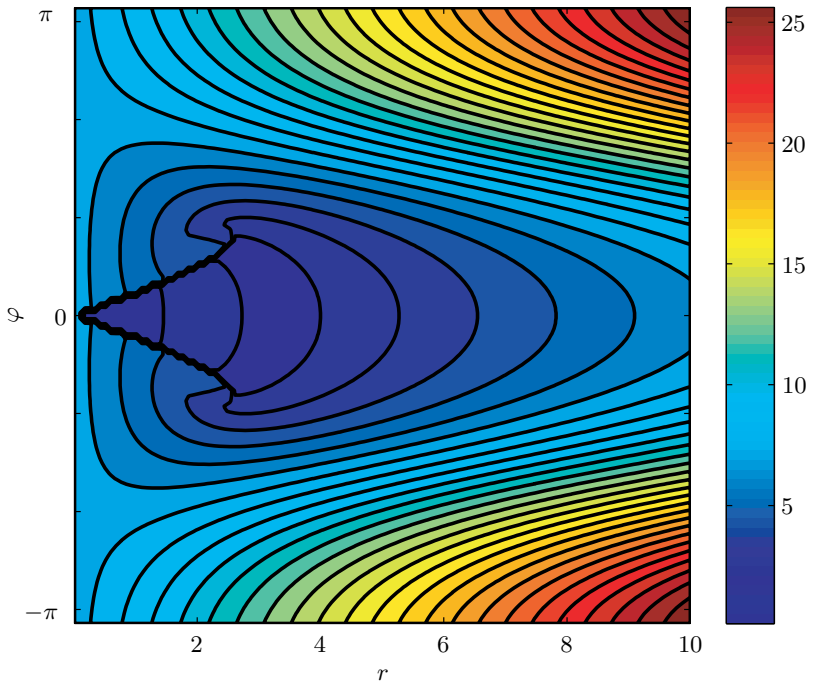


(a) Tailwind ($\gamma = 0$).

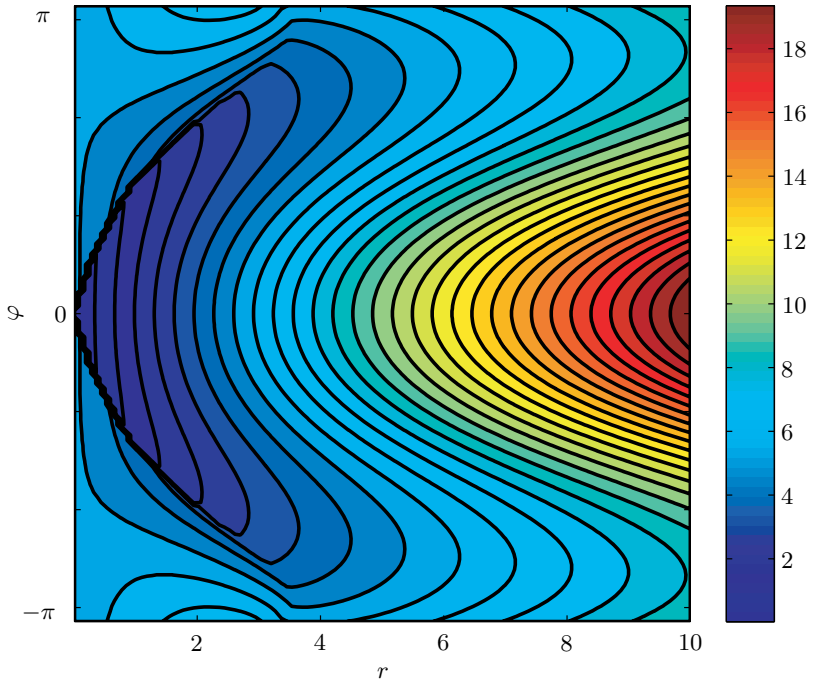


(b) Headwind ($\gamma = \pi$).

**Fig. 8 Level sets of the minimum time-to-go function of the MD problem with free terminal heading in the presence of a constant wind ($\sigma_\theta = 0$).**

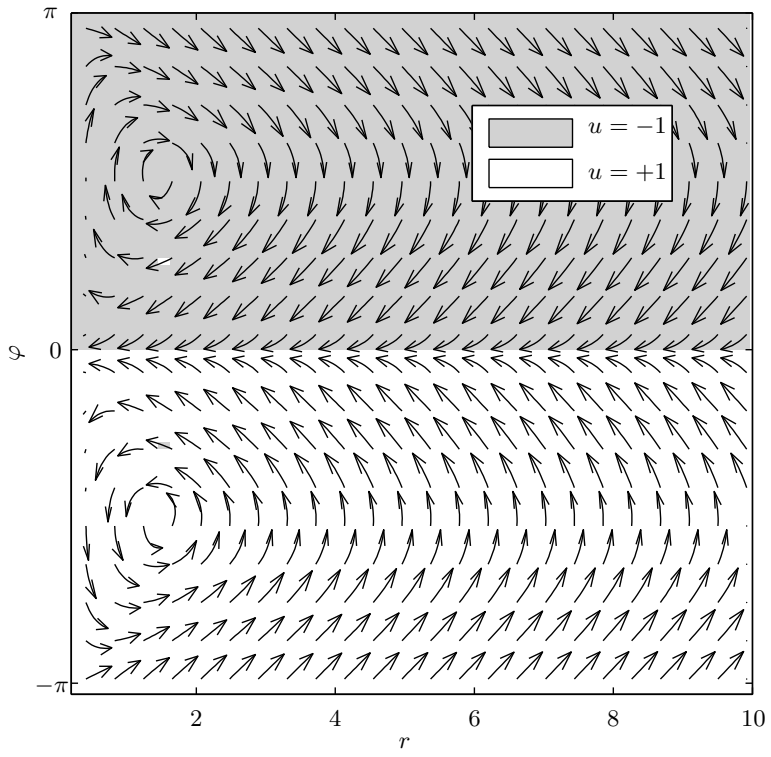


(a) Tailwind ($\gamma = 0$).

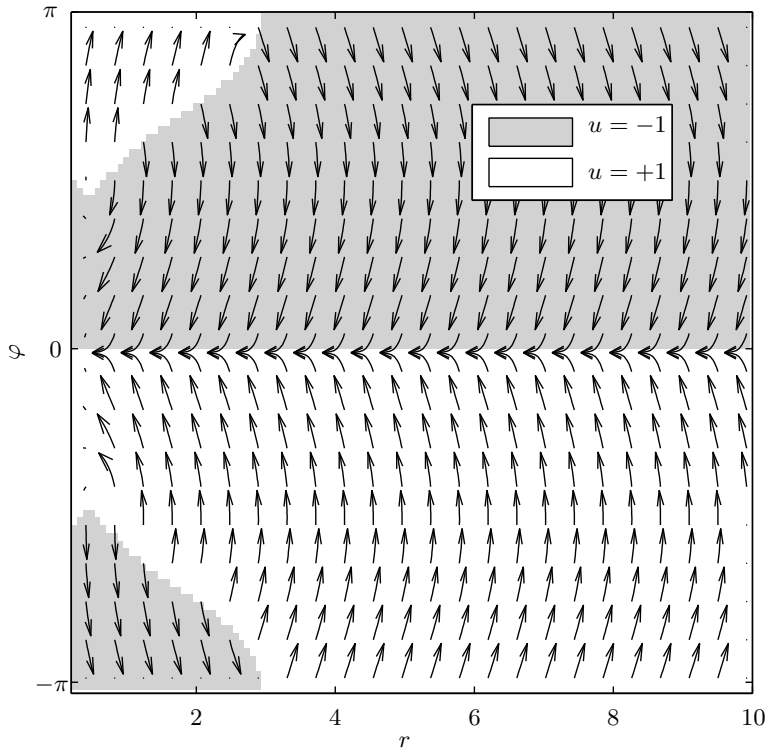


(b) Headwind ($\gamma = \pi$).

**Fig. 9 Dubins vehicle optimal turning rate control policy $u(r, \varphi, \gamma)$ for stochastic model (W2) with $\sigma_\theta = 0.1$.**

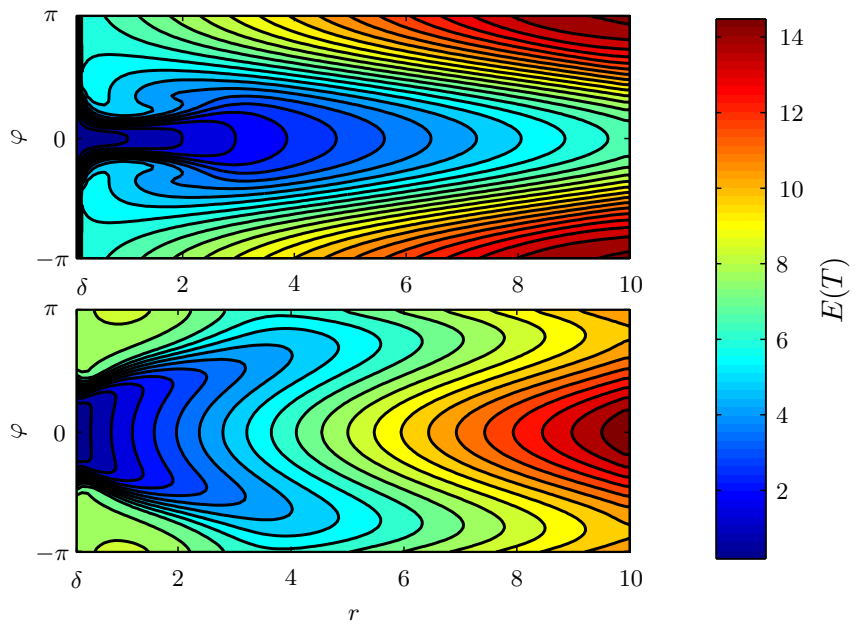


**Fig. 10 Level sets of the minimum time-to-go function of the MD problem with free terminal heading in the presence of a wind with stochastically varying direction and constant speed $v_w$.**

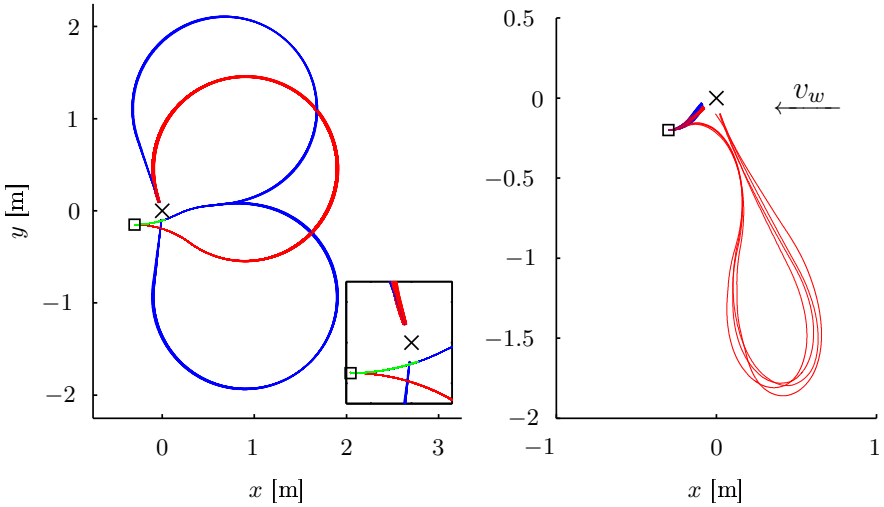


**Fig. 11 DV trajectories for 500 realizations under wind model (W1) (left) and (W2) (right) starting with an initial condition that may result in a difference between trajectories resulting from the control based on the deterministic (red) and stochastic (blue or green) wind models. The initial DV positions are marked with a □, and the target is marked with an ×.**

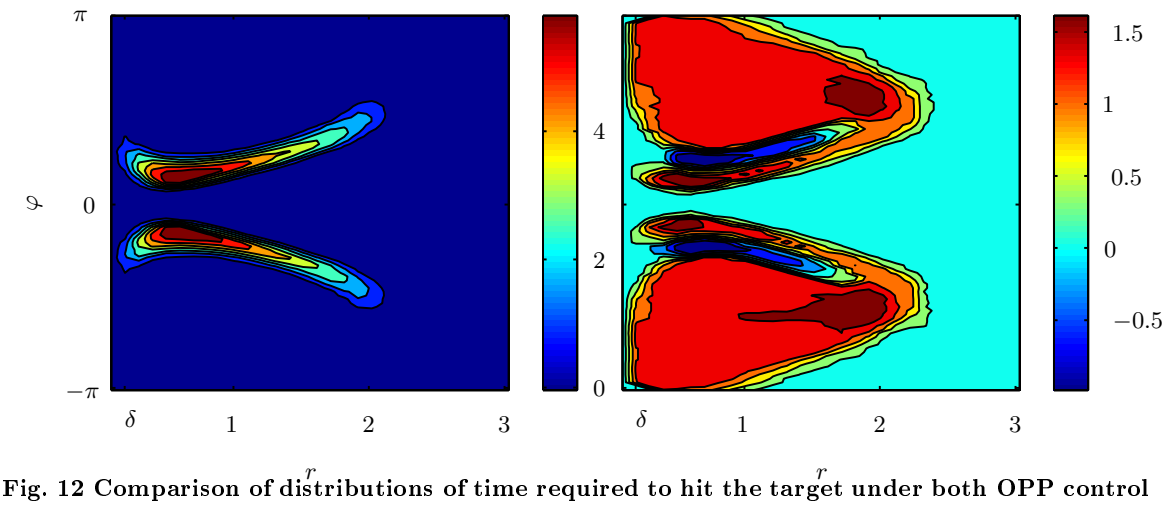


**Fig. 12 Comparison of distributions of time required to hit the target under both OPP control (8) and the stochastic optimal control $u(r,\varphi)$, $\sigma_W = 0.1$ in the presence of the stochastic wind (W1). Left: difference in mean hitting time $\mathbf{E}(T_{\mathbf{OPP}}) - \mathbf{E}(T_{\mathbf{stoch}})$. The OPP control results higher $\mathbf{E}(T)$ in regions where the stochastic model-based control differs from the OPP control. Right: difference in standard deviation $\mathrm{std}(T_{\mathbf{OPP}}) - \mathrm{std}(T_{\mathbf{stoch}})$. As expected, the OPP control results in higher standard deviation in the majority of cases.**

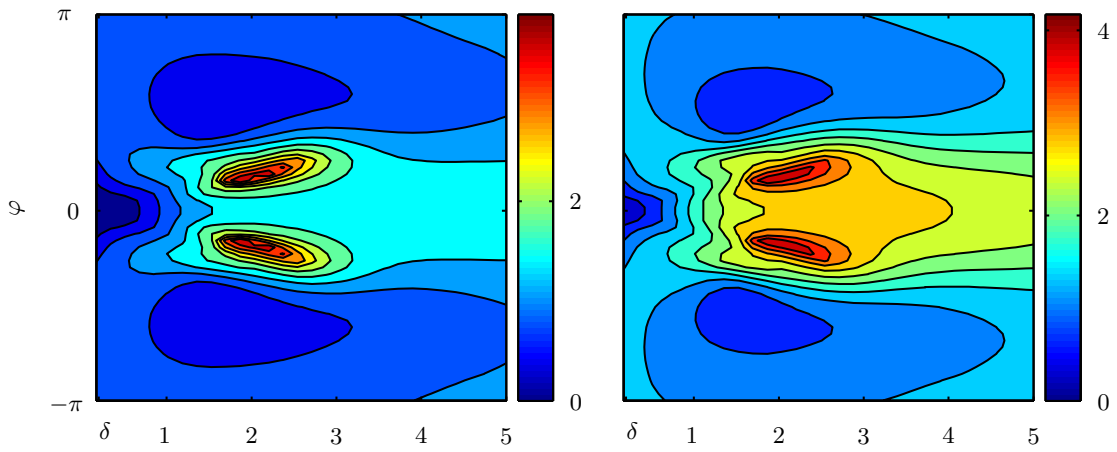


(a) Tailwind ($\gamma = 0$).

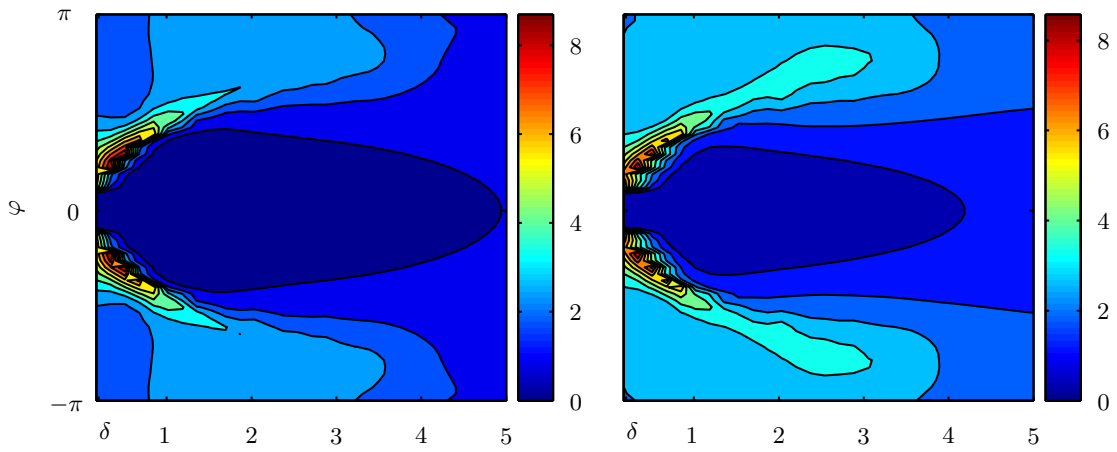


(b) Headwind ($\gamma = \pi$).

**Fig. 13 Comparison of distributions of time required to hit the target under both OPP control (Fig. 6) and the stochastic optimal control (Fig. 9) in the presence of the stochastic wind (W2). Left: difference in mean hitting time $\mathbf{E}(T_{\mathbf{deter}}) - \mathbf{E}(T_{\mathbf{stoch}})$. Right: difference in standard deviation $\mathrm{std}(T_{\mathbf{deter}}) - \mathrm{std}(T_{\mathbf{stoch}})$.**